Sonochemical Deposition and Characterization of Nanophasic Amorphous Nickel on Silica Microspheres

Sivarajan Ramesh,[†] Yuri Koltypin,[†] Ruslan Prozorov,[‡] and Aharon Gedanken*,[†]

Departments of Chemistry and Physics, Bar-Ilan University, Ramat Gan 52900, Israel

Received July 22, 1996. Revised Manuscript Received October 1, 1996[⊗]

Nanophasic, amorphous clusters of elemental nickel in the size range 10−15 nm have been deposited on submicrospheres of amorphous silica by the sonication of a suspension containing nickel tetracarbonyl and silica submicrospheres in Decalin by a high-intensity ultrasound radiation. The nickel-coated silica spheres have been characterized by X-ray, TEM, SEM/EDXA, BET nitrogen adsorption, dynamic light scattering, IR spectroscopy, and magnetic susceptibility measurements. The as-deposited amorphous clusters transform to a polycrystalline, nanophasic, fcc nickel on heating in an inert atmosphere of argon at a temperature of 400 °C. Nitrogen adsorption measurements showed that the amorphous nickel with a high surface area undergoes a loss in surface area on crystallization. Particle size determinations by dynamic light scattering suggested the agglomeration between nickel-coated spheres to be less than that for uncoated spheres. Scanning and transmission electron microscopic investigations revealed the silica spheres coated with polycrystalline nickel to be connected by larger aggregates of nickel (30−40 nm), forming a neck. As-deposited amorphous nickel showed a superparamagnetic behavior, while the polycrystalline nickel on silica was found to be ferromagnetic. FT-IR investigations showed a significant change in the surface silanol composition for the coated and uncoated silica. Ultrasound-driven cavitation desorbs the adsorbed water on silica, making the free silanols available for reaction with nickel species. A positively charged nickel species thus formed could constitute a nucleating site for further aggregation of nickel. An alternate mechanism for the interaction of nickel clusters with the silica surface is proposed, wherein ultrasound irradiation results in the dehydrative condensation of hydrogen-bonded silanols to form siloxane links followed by the formation of a bond between nickel and the bridging oxygen of the siloxane links.

Introduction

The synthesis of ceramics, metals, and alloys in nanoscale dimensions and ceramics coated with nano-sized metal particles has been a topic of active research in recent years due to their wide spanning applications in heterogeneous catalysis, nonlinear optics, and magnetics.[1−3] Particularly the nature of the interaction involved between metal clusters or films and metal oxide surfaces has attracted experimental and theoretical investigations in recent times.[4−6] Metal clusters and thin films deposited by conventional methods such as evaporation and sputtering normally result in a polycrystalline product. The synthesis of amorphous metals and alloys has been limited by the extremely high cooling rates required in the process. Suslick et al. for the first time reported the synthesis of nanophasic, amorphous, elemental iron by a sonochemical method involving the irradiation of iron pentacarbonyl by a high-intensity ultrasound radiation.[7] This method is based on the cavitational phenomena, viz. the formation, growth, and implosive collapse of bubbles in a liquid medium.[8] Extremely high temperatures and very high cooling rates ($>10^7$ K/s) attained during cavitation have been exploited in this method to break the metal carbonyl bonds to form nanophasic amorphous metals. Adopting similar techniques amorphous alloys[9] of cobalt and iron and nanophasic elemental nickel[10] have been synthesized. However, the potential of the sonochemical method as a deposition tool of amorphous metal clusters on morphologically interesting substrates such as single crystals and ceramic microspheres has not been exploited so far. The major advantage of the sonochemical method, apart from a fast quenching rate and operation at ambient conditions is the ability to control the particle size of the product by simply varying the concentration of the metal carbonyls in the soution.[11] In the present work we report the sonochemical deposition and characterization of amorphous, nanophasic nickel particles on the surface of submicrospheres of amorphous silica synthesized by Stober's method.[12] This method provides a relatively simple yet efficient route

[†] Department of Chemistry.
[‡] Department of Physics.
[⊗] Abstract published in *Advance ACS Abstracts,* December 1, 1996.

(1) Ichianose, N. *Superfine particle technology*; Springer-Verlag: Berlin, 1992.
(2) Bloemer, M. J.; Haus, J. W. *Appl. Phys. Lett.* **1992**, *61*, 1619.
(3) Hayashi, T.; Hirono, S.; Tomita, M.; Umemura, S. *Nature* **1996**, *381*, 772.
(4) *Metal-Ceramic Interfaces*; Ruhle, M., Evans, A. G., Ashby, M. F., Hizth, J. P., Eds.; Pergamon: Oxford, 1990.
(5) Di Nardo, N. J. *Nanoscale characterization of surfaces and interfaces*; VCH: Weinheim, Germany, 1994.
(6) Pacchioni, G.; Rosch, N. *J. Chem. Phys.* **1996**, *104*, 7329.
(7) Suslick, K. S.; Choe, S. B.; Cichowlas, A. A.; Grinstaff, M. W. *Nature*, **1991**, *353*, 414.
(8) *Ultrasound: its chemical, physical and biological effects*; Suslick, K. S., Ed.; VCH: Weinheim, Germany, 1988.
(9) Bellisent, R.; Galli, G.; Hyeon, T.; Magazu, S.; Majolino, D.; Miggliardo, P.; Suslick, K. S. *Phys. Scr.* **1995**, *T57*, 79.
(10) Koltypin, Yu.; Katabi, G.; Prozorov, R.; Gedanken, A. *J. Non.-Cryst. Solids* **1996,** *201*, 159.
(11) Cao, X.; Koltypin, Yu.; Kataby, G.; Prozarov, R.; Gedanken, A. *J. Mater. Res.* **1995**, *10*, 2952.

S0897-4756(96)00390-0 CCC: $14.00

to synthesize nanophasic, amorphous metal clusters on supports at ambient conditions. Also the nature of the interaction between amorphous nickel clusters and the surface of amorphous silica has been examined.

Experimental Section

Due to the exceptionally toxic nature of nickel tetracarbonyl, precaution must be taken during its handling.[13] The distillation must be carried out inside a fume cupboard. Carbon monoxide at the outlet must be collected in a second trap connected in series and immersed in a liquid nitrogen bath to be safely disposed later. Consult ref 13 for instructions regarding the safe handling of nickel tetracarbonyl.

Amorphous microspheres of silica were synthesized by a base-catalyzed hydrolysis of tetraethyl orthosilicate (TEOS) in a 1:1 mixture of ethyl alcohol and water by following the procedure described by Stober et al.[12] Ammonium hydroxide was used to catalyze the hydrolysis. Silica microspheres thus obtained were washed extensively with alcohol and ether in a centrifuge and dried in a vacuum. The sonochemical deposition of nickel was carried out as follows: 250 mg of silica was added to 40 mL of Decalin in a sonication cell, stirred well to form a slurry, and connected to the sonicator under flowing argon. Nickel tetracarbonyl (Pfaltz and Bauer) was distilled prior to use at room temperature by bubbling carbon monoxide gas (Mathesson), and the resulting pure $Ni(CO)_4$ was condensed in a cold trap kept immersed in an acetone dry ice bath. Distilled nickel tetracarbonyl (5 mL) was introduced into the sonication cell through a septum. Sonication of the slurry with a high-intensity ultrasound radiation for 1 h was carried out by employing a direct immersion titanium horn (Vibracell, 20 kHz, 100 W/cm^2) under argon at a pressure of approximately 1.5 atm. The sonication cell was kept immersed in a cold bath containing a mixture of acetone and dry ice during the entire sonication. The resulting black product after sonication was washed with *n*-hexane, thoroughly dried in vacuum, and transferred to a glovebox. Earlier DSC measurements[10] have shown that elemental amorphous nickel crystallizes above a temperature of 330 °C. Consequently in a separate experiment 50 mg of the dried black product was heated in special quartz furnace under flowing argon at a temperature of 400 °C for 3 h, and the product stored in a glovebox. X-ray diffraction experiments on the solid products were carried out employing a Rigaku X-ray diffractometer (Model-2028, Cu Kα). Elemental composition by EDXA and morphology by scanning electron microscopy were studied employing a JEOL-JSM 840 scanning electron microscope. Particle morphology and the nature of the nickel deposition on silica was also studied by transmission electron microscopy employing a JEOL-JEM 100SX microscope. Mean particle sizes in a unimodal distribution were determined by dynamic light scattering of the suspension of the particles in ethyl alcohol with a Coulter N4 particle size analyzer. Magnetic susceptibility measurements were carried out by employing a Quantum Design MPMS Squid magnetometer on accurately weighed (ca. 10 mg) samples packed in a gelatin capsule. BET adsorption of nitrogen was carried out employing a Micromeritics surface area analyzer. Infrared spectra were recorded employing a Nicolet (impact 410) FT-IR spectrometer by a KBr disk method.

Results and Discussion

The mixture containing the reactants turned black within few minutes of irradiation with ultrasound. The sonication cell was kept much below ambient temperature (<−50 °C) to avoid the possibility of thermal deposition of nickel from the carbonyl. In the absence of ultrasound no deposition of nickel occurred. Figure 1 shows the X-ray diffractograms of the (a) uncoated Stober's silica, (b) silica coated with as-deposited nickel, and (c) the nickel-coated silica subjected to heating in argon at 400 °C for 3 h. Uncoated silica and silica coated with as-deposited nickel were found to be X-ray amorphous as evident from the presence of a broader hump in the XRD pattern. The amorphous nature of the elemental nickel further confirms that the decomposition of nickel tetracarbonyl was due to cavitation induced by ultrasound and not due to thermal effects. The sample heated in argon showed diffraction peaks of ⟨111⟩ and ⟨200⟩ planes characteristic of polycrystalline, fcc form of elemental nickel suggesting the amorphous to crystalline transformation of the as deposited nickel. Figure 2a shows the representative transmission electron micrograph of the as prepared Stober's silica. The particles were spherical with a narrow size distribution with an average diameter of approximately 250 nm. Figure 2b shows the TEM micrographs of silica coated with amorphous nickel. Spongy agglomerates of nickel suspended in the solution could also be seen in this picture. Magnified TEM image of a single silica sphere deposited with amorphous nickel on the surface is shown in Figure 2c. Small nickel particles in the size range 10−15 nm could be seen clearly on the surface of amorphous silica. TEM micrographs of silica sample coated with polycrystalline nickel is shown in Figure 2d. Spongy agglomerates of nickel could not be found in these samples. This is expected as heating at 400 °C can result in the sintering of the spongy agglomerates of amorphous nickel into a dense, polycrystalline particle. Also silica spheres were observed to be interconnected by means of spherical globules of polycrystalline metallic nickel.

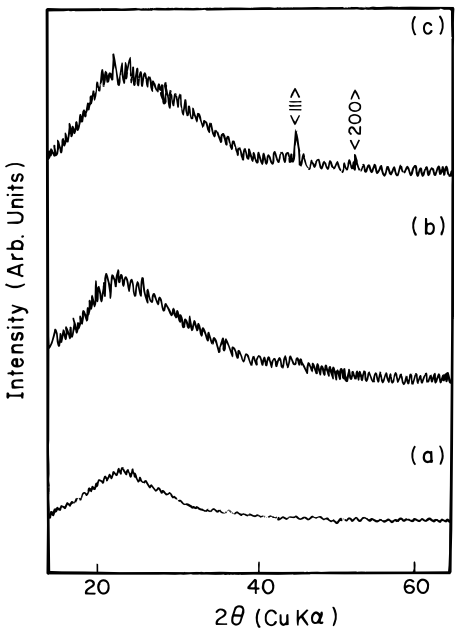

Figure 1. X-ray diffractograms of (a) amorphous silica, (b) silica coated with amorphous nickel, and (c) silica coated with polycrystalline nickel.

The Energy Dispersive X-ray Analysis (EDXA) results for the uncoated and amorphous nickel coated silica are shown in Figure 3, parts a and b, respectively. The relative intensities of silicon and oxygen are the same in both samples, thus verifying that the oxygen signal

(12) Stober, W.; Fink, A.; Bohn, E. J. *Colloid Interface Sci.* **1968**, *26*, 62.

(13) (a) Brauer, G. Handbook of preparative inorganic chemistry; Academic Press: New York, 1965; Vol. 2. (b) Jolly, P. W. In *Comprehensive Organometallic Chemistry*; Wilkinson, G., Stone, F. G. A., Abel, E. W., Eds.; Pergamon: New York, 1982; Vol. 6.

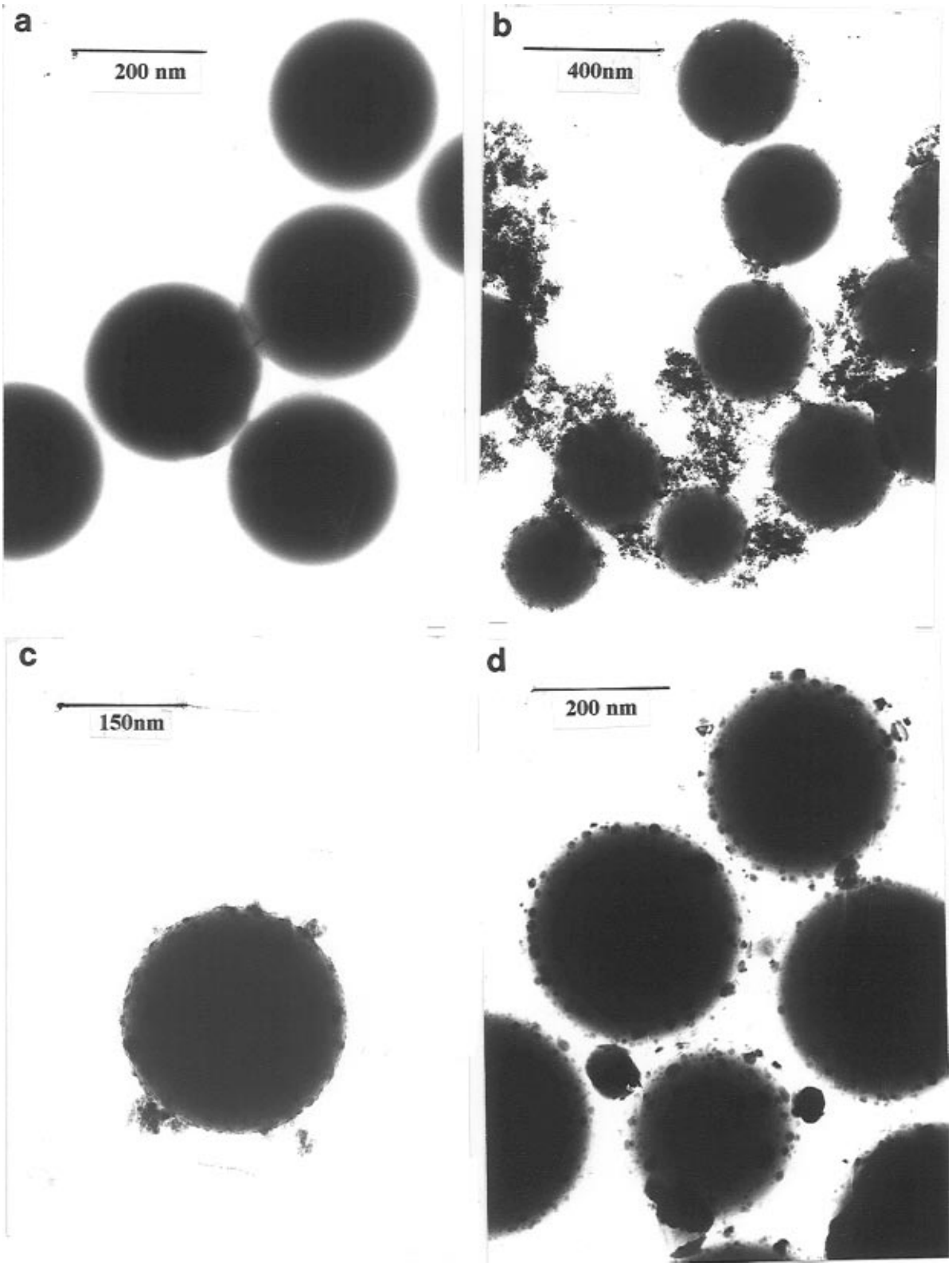

Figure 2. Transmission electron micrographs of (a) silica microspheres, (b) silica with amorphous, nanophasic nickel adhering to the surface, (c) magnified image of a single silica sphere with amorphous nickel on the surface, and (d) silica microspheres with polycrystalline nanophasic nickel adhering to the surface.

is due to the oxygen in silica. This confirms the elemental nature of amorphous nickel and rules out the presence of any additional oxide impurities. The intensity ratio of the nickel peak was approximately 40% to that of silica. The values of the surface area (BET nitrogen adsorption) and particle sizes estimated by dynamic light scattering for all the three samples are listed in Table 1. The lower value of the surface area for Stober's silica at 9.69 m^2/g is comparable to those reported in the literature and can be understood in terms of a hydrogen-bonded network of surface silanols which decrease the accessibility of the silica surface for the probing gas (N_2). However, the surface area of silica coated with amorphous nickel showed an increase of about 200% attributable to spongy amorphous nickel clusters coated on silica. Crystallization of amorphous

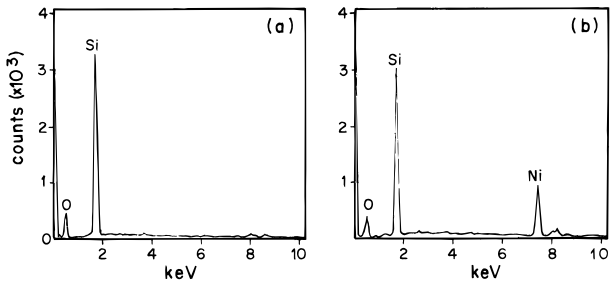

Figure 3. EDXA profiles for (a) Stober's silica and (b) silica deposited with amorphous nickel.

Table 1. Surface Area by BET Nitrogen Adsorption, Mean Particle Diameter by Dynamic Light Scattering, and the Magnetic Coefficients[a] for Amorphous and Polycrystalline Nickel on Silica

parameter	uncoated silica	amorphous Ni/SiO_2	polycrystalline Ni/SiO_2
surface area BET (M^2/g)	9.69	28.13	11.84
mean diameter (DLS) nm	497.8	386.6	1974
σ_1		25.293	19.465
σ_2		−191.253	−125.33
ϕ_1		3.201×10^{-3}	0.1323
ϕ_2		3.113×10^{-5}	-1.425×10^{-3}
R^2		0.9971	0.9964

[a] σ_i and ϕ_i are the coefficients in the expression $M_H = M_{0,RT}\{1 - (\sigma_1/\sqrt{H}) - (\sigma_2/H) - (\sigma_3/\sqrt{H^3}) - ...\} + \phi_1\sqrt{H} + \phi_2 H$ fitted to the experimental data describing the nature of the interface magnetization. R^2 is the residual parameter which has a value of 1 for an ideal fit.

nickel was accompanied by a drastic decrease in surface area, which can be understood in terms of the aggregation and sintering of reactive metal clusters under the influence of heat. Crystallization of nanophasic amorphous nickel below 400 °C has been confirmed in our earlier study[10] with the aid of differential scanning calorimetry. The above observations were also supported by particle size measurements. Particle size measurements by dynamic light scattering showed some interesting changes in the mean diameter of the coated and uncoated particles, while the same parameter measured by TEM remained essentially unchanged. The values of mean diameter of uncoated spherical silica measured by dynamic light scattering (497 nm) is considerably higher than the values observed by TEM. This can be attributed to the agglomeration of a fraction of silica spheres in the dispersant medium. Interestingly silica spheres coated with amorphous nickel showed a mean diameter lesser than the uncoated silica spheres. This could be explained in two ways, viz., the agglomerating tendency of silica spheres deposited with an amorphous nickel decreases and hence can cause a decrease in the mean diameter values. On the other hand, the undeposited, spongy nickel agglomerates can also contribute to the fall in the mean diameter values. While it is difficult to attribute any one of these processes solely to the decrease in the mean diameter, an interplay of both these effects cannot be ruled out. The unusually high mean particle sizes measured (<1900 nm) in the case of silica coated with polycrystalline nickel can be understood only in terms of the interconnection of silica spheres through the formation of necks by agglomerated sintered nickel particles which are viewed as large particles in a light-scattering method. However, TEM studies could clearly confirm the interconnection of silica spheres by means of nickel metal aggregates.

The magnetization loops for the amorphous and polycrystalline nickel deposited on silica are shown in Figure 4, parts a and b, respectively. Amorphous nickel did not show a hysteresis loop, whereas the polycrystalline nickel on silica showed a hysteresis loop ($M_r/M_s = 0.233$) characteristic of a ferromagnet. The absence of ferromagnetism in amorphous nickel can be ascribed to the absence of long-range order.[14] The variation of normalized magnetization (M_H/M_S) as a function of the applied field (for $H \leq 15\,000$ Oe) for both the nickel samples is shown in Figure 5a. Magnetic saturation was reached at lower fields (<2.5 kOe) in the case of the polycrystalline nickel, whereas the rate of magnetization was slower in the case of amorphous nickel. This could be attributed to a difference in the size distribution of nickel particles in both the samples. The slow approach to saturation magnetization due to nanophasic dimensions of the magnetic particles have been recently reported in the case of cobalt ferrites[15] and carbon-coated nanophasic cobalt, iron, and nickel.[16] The nickel-coated silica samples were treated as a magnetic mass having the same amount of nickel per silica sphere in the case of amorphous and polycrystalline materials. The specific magnetization was calculated including the weight of the silica core. The effect of a silica core and a silica−nickel interface on the magnetization behavior of the samples was analyzed by following the approach of Wang et al.[17] Magnetization values as a function of applied field (H) were fitted to the expression

$$M_H = M_{0,RT}\{1 - (\sigma_1/\sqrt{H}) - (\sigma_2/H) - (\sigma_3/\sqrt{H^3}) - ...\} + \phi_1\sqrt{H} + \phi_2 H \quad (1)$$

by a method of nonlinear regression by least-squares minimization. In eq 1 M_H is the observed magnetization and $M_{0,RT}$ is the magnetization value at room temperature, H is the field strength expressed in Oersteds. σ_i and ϕ_i are the coefficients which give information about the magnetization processes at the interface. The fitting was not good in the case of polycrystalline nickel/silica at higher fields as the saturation was reached at much lower field. However, excellent fitting could be obtained for $H \leq 5000$ Oe. Optimized values were obtained for the coefficients σ_i and ϕ_i in the case of both amorphous and polycrystalline nickel. Experimental and calculated values of magnetization as a function of H are shown in Figure 5b and the coefficients are listed in Table 1. The $1/\sqrt{H}$ term is identified with an inhomogeneous spin structure in the interfacial region[17] and the values of σ_1 in the case of amorphous and polycrystalline nickel are comparable, suggesting that the degree of inhomogeniety may be of the same order in both the samples. A negative value of ϕ_2 in the case of polycrystalline nickel on silica can be attributed to a greater diamagnetic contribution[17] from the silica core in the case of polycrystalline nickel/silica. This observation suggests that the nickel−silica interaction in the case of polycrystalline sample may be stronger than in the case of amorphous nickel on silica.

(14) Kaneyoshi, T. *Amorphous magnetism*; CRC Press: Boca Raton, FL, 1984.
(15) Moumen, N.; Pileni, M. P. *J. Phys. Chem.* **1996**, *100*, 1867.
(16) Jiao, J.; Seraphin, S.; Wang, X.; Withers, J. C. *J. Appl. Phys.* **1996**, *80*, 103.
(17) Wang, W. N.; Cheng, G. X.; You, W. D. *J. Magn. Magn. Mater.* **1996**, *153*, 11.

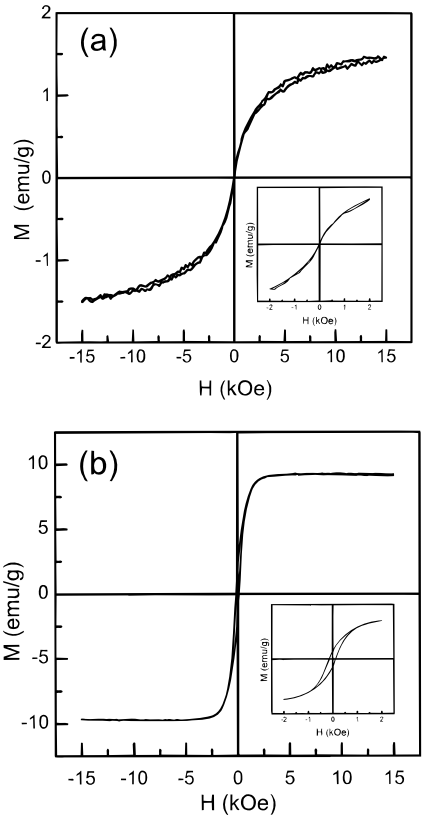

Figure 4. (a) $M-H$ curve for amorphous nickel on silica and (b) hysteresis loop shown by polycrystalline nickel on silica ($M_r/M_s = 0.233$). Inset in both the figures show the M−H behavior in the lower magnetic field range.

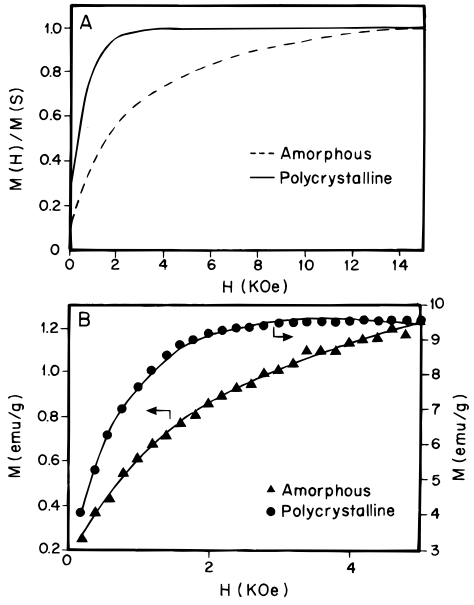

Figure 5. (a) Normalized magnetization as a function of magnetic field for amorphous and polycrystalline nickel on silica microspheres. (b) Observed magnetization and the values calculated from eq 1 as a function of increasing magnetic field H: (▲) amorphous nickel on silica; (●) polycrystalline nickel on silica. Solid lines represent the calculated values.

Infrared spectra of the uncoated Stober's silica, silica coated with amorphous nickel, and silica coated with polycrystalline nickel particles are shown in Figure 6a−c, respectively. The IR spectra of the uncoated silica matched well with the spectra reported in the literature.[18] The uncoated Stobers's silica showed three

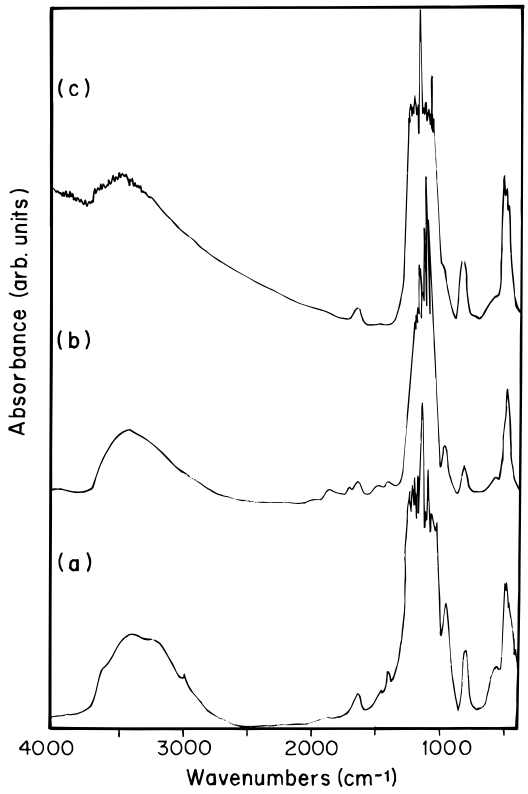

Figure 6. FT-IR spectra of (a) amorphous silica microspheres, (b) silica deposited with amorphous, nanophasic nickel, and (c) silica deposited with polycrystalline nickel.

distinct features in the −OH stretching region (2800−3800 cm^{-1}) viz., 3650, 3420, and 3220 cm^{-1}. These bands could be assigned to internal silanols and hydrogen-bonded surface silanols. The shoulder at 3650 cm^{-1} is absent in the case of silica coated with amorphous nickel. Also a decrease in the relative intensity of the band at 3220 cm^{-1} was observed. The absence of a strong absorption above 3700 cm^{-1} is indicative of the absence of free surface silanols in the case of Stober's silica which has been recognized as a characteristic of ethyl silicate derived silicas.[18,19] Burneau et al.,[18] while studying the effect of thermal dehydration of silica of different origins observed that the decrease in the intensity of the bands in the range 3200−3300 cm^{-1} was due to the breaking of silanol water bonds. Such a process would expose the metal to free silanols on the silica surface.

The nature of the interaction between elemental metals liberated from carbonyls and the −OH groups on hydroxylated surfaces have been investigated earlier.[20,21] Hucul and Brenner[20] have studied the temperature-programmed decomposition of various metal carbonyls on an alumina surface and proposed that the −OH species on the surface reacts with elemental metals to form an oxidized metal species of the type Al−O−$M^{\delta+}$ with the liberation of hydrogen. Basu et al.[21] have examined the thermolysis of rhodium carbonyl on the surface of alumina and presented the first and direct

(18) Burneau, A.; Barres, A.; Gallas, J. P.; Lavalley, J. C. *Langmuir* **1990**, *6*, 1364.
(19) Kondo, S.; Muroya, M.; Fujii, K. *Bull. Chem. Soc. Jpn.* **1974**, *47*, 553.
(20) Hucul, D. A.; Brenner, A. *J. Phys. Chem.* **1981**, *85*, 496.
(21) Basu, P.; Panyotov, D.; Yates, J. T., Jr. *J. Am. Chem. Soc.* **1988**, *110*, 2074.

spectroscopic evidence for the disruptive oxidation of small rhodium crystallites to form oxidized rhodium species. On similar lines, Ni^0 fragments may be expected to react with the free surface silanols on the surface of Stober's silica to form $Si-O-Ni^{\delta+}$ species, which in turn may serve as a nucleating site for the further aggregation of nickel. However, under the influence of ultrasound an alternate mechanism for the interaction of nickel with silica surface is possible as discussed below.

Pacchioni et al.[6] have recently carried out an extensive quantum-chemical investigation of the interaction of small metal clusters such as Ni and Cu with an insulating oxide surface of single-crystal magnesia. They have observed that the oxidizing capability of the surface oxygen is an important parameter in the formation of an interface bond. The nature of the interaction between metallic nickel and the oxide surface was found to be the formation of a covalent polar bond formed by the mixing of the 3d orbitals of nickel with O2p bands of the oxide. Johnson and Pepper[22] have also shown by means of a cluster model and molecular orbital theory that a direct and primarily covalent chemical bond can be established between elemental metals such as Fe, Ni, Cu, and Ag and the oxygen anions on the surfaces of clean sapphire. On the basis of the above observations, formation of a moderately strong chemical bond between a surface oxide species on silica and nickel can reasonably be assumed. The surface of silica contains mainly four types of oxygen species, viz. the oxygen associated with (a) single free silanols, (b) oxygen in the network of hydrogen-bonded silanols, and (c) silanol oxygens bonded to physisorbed water, and (d) the bridging oxygen in the siloxane links. The lesser reactivity to adsorb probing gases has been established in the case of hydrogen bonded silanols.[18] The hydrogen-bonded network can be broken by powerful ultrasound radiation to form siloxane links, and the bridging oxygen in the siloxane link can now form a reactive adhesion site for the adsorption of nickel clusters. This view is strengthened by the IR observations which show a decrease in the relative intensity of the band at 3220 cm^{-1}. In an earlier investigation[23] we have shown that high-intensity ultrasound can disrupt the hydrogen-bonded network on the surface of Stober's silica resulting in their dehydrative condensation. Thus ultrasound induced cavitation seems to play a dual role of breaking the nickel carbonyl bonds as well as activating the amorphous silica surface for adhesion of nickel. In an interesting nuclear-spin cross-polarization dynamics study of the hydrated and evacuated samples of silica, Chuang and Maciel[24] observed that the formation of a Si−O−Si link between two surface silanols is facilitated by the hydrogen bonding. Stober's silica with an extensive hydrogen-bonded network on the surface can be expected to be more facile in the formation of siloxane links under the influence of ultrasound radiation. The bridging oxygen in the siloxane links thus can be expected to form a moderately strong chemical bond with nickel atoms. High-energy spectroscopic studies and investigations by atomic force microscopy for a better understanding of the nickel silica interface are underway.

Conclusions

Deposition of amorphous nickel particles on microspheres of silica has been accomplished by a sonochemical method. Cavitation induced by a high-intensity ultrasound radiation is suggested to result in the breaking of nickel−carbonyl bonds as well as activating the silica surface for adhesion of nickel through the formation of siloxane links. An alternate mechanism involves the reaction of nickel metal with the surface silanols freed from adsorbed water by cavitation to form positively charged nickel on the silica surface. These $Si-O-Ni^{\delta+}$ sites could serve as nucleating centers for the further agglomeration of nickel. Nanophasic amorphous nickel was found to be superparamagentic, whereas crystallization resulted in a ferromagnetic material showing a stronger nickel−silica interaction. These materials promise to have potential applications in magentism and heterogeneous catalysis.

Acknowledgment. A.G. thanks the Ministry of Science and Technology for supporting this research through the grants for infrastructure. Y.K. thanks the Ministry of Absorption for his Giladi scholarship. The authors thank Professor M. Deutsch, Department of physics, for extending the XRD facility.

CM960390H

(22) Johnson, K. H.; Pepper, S. V. *J. Appl. Phys.* **1982**, *53*, 6634.
(23) Ramesh, S.; Koltypin, Yu.; Gedanken, A., communicated.
(24) Chuang, I. S.; Maciel, G. E. *J. Am. Chem. Soc.* **1996**, *118*, 401.